ISME

Vibration Analysis of a Double Layer Microshell Utilizing a Modified Couple Stress Theory

J. Ehyaei[*]
Assistant Professor

H. Safarpour[†]
Master of Science

E.Shahabinejad[‡]
Master of Science

In this paper, dynamic modeling of a double layer cylindrical functionally graded (FG) microshell is considered. Modeling is based on the first-order shear deformation theory (FSDT), and the equations of motion are derived using the Hamilton's principle. It assumes that functionally graded length scale parameter changes along the thickness. Generalized differential quadrature method (GDQM) is used to discretize the model and solve the problem. In this research the size effect is investigated using a new modified couple stress theory (MCST) which has been considered for the first time in the present study. The accuracy of the presented model is validated with some cases in the literature. Considering the microshell as double layer and utilizing the MCST in addition to considering the various boundary conditions are the novelty of this study. Furthermore, the effects of length, thickness, FG power index, Winkler and Pasternak coefficients and shear correction factor on the natural frequency of double layer cylindrical FG microshell are studied.

Keywords: Double walled; Functionally graded material; Moderately thick cylindrical microshell; Modified couple stress theory; Vibration analysis.

1 Introduction

The applications of FG cylindrical shells are very broad. They can be applied to Functionally graded materials (FGMs) have many advantages and superior properties, including high temperature fuselage structures of civil airliners, aerospace structures, military aircraft propulsion system, and other engineering fields. In addition, the investigation of their vibration characteristics is of great interest for design engineers and manufactures. Haddadpour et al. [1] and Farid et al. [2] investigated the vibration of cylindrical FG shells and panels. Moreover, the use of FG materials has received a considerable attention within the micro/nano structures such as atomic force microscopes, Rahaeifard et al. [3] and micro/nano electromechanical systems, lee et al. [4], Ghasemabadian et al. [5].

[*]Corresponding Author, Assistant Professor, Faculty of Engineering, Department of Mechanics, Imam Khomeini International University, Postal code: 34148 - 96818, Qazvin, Iran jehyaei@eng.ikiu.ac.ir
[†] Master of Science, Faculty of Engineering, Department of Mechanics, Imam Khomeini International University, Postal code: 34148 - 96818
[‡] Master of Science, Faculty of Engineering, Department of Mechanics, Imam Khomeini International University, Postal code: 34148 – 96818
Receive : 2019/03/13 Accepted : 2019/10/20

Here, it should be noted that when the sizes change to the nano /micro scale, new phenomena are created. In the micro/nano scales, the material properties depend on the micro/nano scale. Cylindrical shells have been widely used in micro- and nano-scale devices and systems. It should be noted that the size effect is not important in the classical continuum theories while it cannot be overlooked for micro and nano scale systems. One of the non-classical theories that consider the effect of size is couple stress theory. Koiter [6], and Mindlin[7] investigated the couple stress theory including higher order rotation gradients, which is in fact the asymmetric part of the deformation gradient. According to this theory, there are four material constants (two classical and two additional) for isotropic elastic materials. Asghari et al. [8] presented the size effects in Timoshenko beams on the basis of the couple stress theory. It is difficult to determine the microstructure related length scale parameters. Therefore, we are looking for the continuum theory which contains only one additional material parameter of length scale. Modified couple stress theory is one of the best and most well-known continuum mechanics theories that include small scale effects with reasonable accuracy in micro scale devices. Yang et al. [9] presented a modified couple stress theory, in which the couple stress tensor is symmetric and only one internal material length scale parameter is involved, unlike the classical couple stress theory mentioned above. Many scholars have used this theory to examine the dynamic and static behavior of micro-beams and micro-plates, Shaat et al. [10].
It is noted that, nonlocal theory of Eringen is one of the famous continuum mechanics theories that includes small scale effects with good accuracy in nano/micro scale devices, although the results show that the modified couple stress theory coincides with experimental results better than Eringen's nonlocal elasticity and classical theories [7] Miandoab et al. [11]. Therefore, in this study, the modified couple stress theory has been used. Unique mechanical properties and extreme electrical conductivity of double-cylindrical shell structures have caused them to be of extensive use in various nanodevices. It is worth mentioning that, dynamic behavior of double walled carbon tubes (DWCNTs) is similar to double cylindrical shell structures. Considering the use of DWCNTs in conveying fluids in nanodevices and the importance of identification of fluid-conveying DWCNTs, many researchers attempt to scrutinize the dynamic behavior of these nanostructures, Karami el *al.* [12], Choi et al. [13], Chang [14]. Recently, zhang et al. [15] studied the free and forced vibration analysis of circular cylindrical double-shell structures under arbitrary boundary conditions. The natural frequencies and mode shapes of the structures as well as frequency responses under forced vibration obtained with the Rayleigh–Ritz procedure. The novelty of this work is consideration of the size effect in the dynamic behavior of double moderately thick cylindrical FG microshell. The main idea of the present work is to propose a numerical model to study the free linear vibration of double FG micro shell using a new modified couple stress theory. Furthermore, GDQM is used to get the numerical results.

In this study the outer and inner cylindrical microshell material is functionally graded material and according to the power law distribution. It is assumed that the outer surface is metal and the inner surface is ceramic. The governing equations and boundary conditions have been developed using Hamilton's principle. The results show that, length, thickness, FG power index, winkler and pasternak coefficients and shear correction factor play important roles on the natural frequency of double cylindrical FG microshell.

2 Mathematical formulations

At the outer and the inner surfaces, the functionally graded nanoshell is generally composed of two different materials. According to the power law distribution, bulk elastic modulus E(z) and mass density $\boldsymbol{\rho}(z)$ are assumed to be change along the thickness direction. Volume fraction index *m* determines the variation profile of material properties across the thickness of

the FG nanoshell. Assuming that the inner surface (at z=−h/2) is metal and the outer surface (at z=h/2) is ceramic, and for different values of *m*, the mechanical properties can be obtain as [16]

$$E(z) = (E^{out} - E^{in})(\frac{z}{h} + \frac{1}{2})^m + E^{in}$$
$$\rho(z) = (\rho^{out} - \rho^{in})(\frac{z}{h} + \frac{1}{2})^m + \rho^{in} \quad (1)$$

According to the first order shear deformation theory, the displacement field of cylindrical shell along the three directions of x,θ and z is expressed as [17]:

$$U(x,\theta,z,t) = u(x,\theta,t) + z\psi_x(x,\theta,t)$$
$$V(x,\theta,z,t) = v(x,\theta,t) + z\psi_\theta(x,\theta,t) \quad (2)$$
$$W(x,\theta,z,t) = w(x,\theta,t)$$

In Eq. (1), u(x,θ,t), v(x,θ,t), and w(x,θ,t) are considered as neutral axis displacement, and ψ_θ(x,θ,t) and ψ_x(x,θ,t) as rotation of a transverse normal surface about the circumferential and axial directions. According to this theory, the strain energy is expressed as [16]:

$$U = \frac{1}{2}\iiint_V (\sigma_{ij}\varepsilon_{ij} + m_{ij}^s \chi_{ij}^s) dV \quad (3)$$

In Eq. (2), χ_{ij}^s, ε_{ij}, σ_{ij} and m_{ij}^s are the components of symmetric rotation gradient tensor, strain tensor, stress tensor, and higher order stress tensor, respectively. Which are expressed as [16]:

$$\varepsilon_{ij} = \frac{1}{2}(u_{,j} + u_{,i}) \quad (4)$$

$$\chi_{ij}^s = \frac{1}{2}(\varphi_{,j} + \varphi_{,i}) \quad (5a)$$

$$m_{ij}^s = 2l^2\mu\chi_{ij}^s, \varphi_i = \frac{1}{2}[curl(u)]_i \quad (5b)$$

It is worth noting that, index *i* and *j* in Eqs. (3), (4), (5a) and (5b) are *x*, θ and *z*, respectively. Also, in the above equations *u* and φ represent the components of displacement vector and infinitesimal rotation vector, respectively. In Eq. (5b), *l* is a parameter which denotes an additional independent material length-scale parameter related to the symmetric rotation gradients. The functionally graded length scale parameter in the cylindrical FG microshells has been considered for the first time in this study. This parameter changes along the thickness.

2.1 Governing equations and boundary conditions

The principle of minimum potential energy states that:

$$\int_{t_1}^{t_2} (\delta T - \delta U + \delta W) dt = 0 \quad (6)$$

The strain energy variation of the structure can be obtained as follows:

$\delta\Pi = \delta U_1 + \delta U_2$:

$$\delta U_1 = \frac{1}{2}\iiint_V (\sigma_{ij}\delta\varepsilon_{ij})dV = \iint_A \left\{ \begin{array}{l} (N_{xx}\frac{\partial}{\partial x}\delta u + M_{xx}\frac{\partial}{\partial x}\delta\psi_x) + N_{\theta\theta}(\frac{1}{R}\frac{\partial}{\partial\theta}\delta v + \frac{\delta w}{R}) + \\ M_{\theta\theta}\frac{1}{R}\frac{\partial}{\partial\theta}\delta\psi_\theta + Q_{xz}(\delta\psi_x + \frac{\partial}{\partial x}\delta w) + \\ N_{x\theta}(\frac{1}{R}\frac{\partial}{\partial\theta}\delta u + \frac{\partial}{\partial x}\delta v) + M_{x\theta}(\frac{1}{R}\frac{\partial}{\partial\theta}\delta\psi_x + \frac{\partial}{\partial x}\delta\psi_\theta) \\ +Q_{z\theta}(\delta\psi_\theta + \frac{1}{R}\frac{\partial}{\partial\theta}\delta w - \frac{\delta v}{R}) \end{array} \right\} R dx d\theta$$

$$\delta U_2 = \frac{1}{2}\iiint_V (m_{ij}^s\delta\chi_{ij}^s)dV = \iint_A \left\{ \begin{array}{l} (-\frac{Y_{\theta\theta}}{2R^2} + \frac{Y_{zz}}{2R^2})\frac{\partial}{\partial\theta}\delta u - (\frac{Y_{\theta z}}{2R^2})\frac{\partial^2}{\partial\theta^2}\delta u - (\frac{Y_{zx}}{2R})\frac{\partial^2}{\partial\theta\partial x}\delta u \\ +(\frac{Y_{\theta\theta}}{2R} - \frac{Y_{xx}}{2R})\frac{\partial}{\partial x}\delta v + (\frac{Y_{xz}}{2})\frac{\partial^2}{\partial x^2}\delta v - (\frac{Y_{\theta x}}{2R^2})\frac{\partial}{\partial\theta}\delta v \\ +(\frac{Y_{\theta z}}{2R})\frac{\partial^2}{\partial\theta\partial x}\delta v + (\frac{Y_{xz}}{2R^2})\delta v + (\frac{Y_{\theta z}}{2R})\frac{\partial}{\partial x}\delta w - (\frac{Y_{\theta x}}{2})\frac{\partial^2}{\partial x^2}\delta w \\ -(\frac{Y_{zx}}{2R^2})\frac{\partial}{\partial\theta}\delta w + (\frac{Y_{x\theta}}{2R^2})\frac{\partial^2}{\partial\theta^2}\delta w + (-\frac{Y_{\theta\theta}}{2R} + \frac{Y_{xx}}{2R})\frac{\partial^2}{\partial\theta\partial x}\delta w \\ +(\frac{Y_{x\theta}}{2})\frac{\partial}{\partial x}\delta\psi_x + (\frac{Y_{\theta\theta}}{2R} - \frac{Y_{xx}}{2R})\frac{\partial}{\partial\theta}\delta\psi_x - (\frac{T_{zx}}{2R})\frac{\partial^2}{\partial\theta\partial x}\delta\psi_x \\ -(\frac{Y_{z\theta}}{2R})\delta\psi_x - (\frac{Y_{x\theta}}{2R})\frac{\partial}{\partial\theta}\delta\psi_\theta + (\frac{Y_{\theta\theta}}{2R} - \frac{Y_{xx}}{2} + \frac{Y_{zz}}{2})\frac{\partial}{\partial x}\delta\psi_\theta \\ +(\frac{T_{z\theta}}{2R})\frac{\partial^2\delta\psi_\theta}{\partial\theta\partial x} - (\frac{T_{z\theta}}{2R^2})\frac{\partial^2\delta\psi_x}{\partial\theta^2} + (\frac{T_{xz}}{2})\frac{\partial^2\delta\psi_\theta}{\partial x^2} - \frac{Y_{xz}}{2R}\delta\psi_\theta \end{array} \right\} R dx d\theta \quad (7)$$

Where the classical and non-classical force and momentum are defined as below:

$$\begin{aligned} &(N_{xx}, N_{\theta\theta}, N_{x\theta}) = \int_{-h/2}^{h/2}(\sigma_{xx}, \sigma_{\theta\theta}, \sigma_{x\theta})dz, \\ &(M_{xx}, M_{\theta\theta}, M_{x\theta}) = \int_{-h/2}^{h/2}(\sigma_{xx}, \sigma_{\theta\theta}, \sigma_{x\theta})zdz, \\ &(Q_{xz}, Q_{z\theta}) = \int_{-h/2}^{h/2}k_s(\sigma_{xz}, \sigma_{z\theta})dz, \\ &(Y_{xx}, Y_{\theta\theta}, Y_{zz}, Y_{x\theta}, Y_{xz}, Y_{z\theta}) = \int_{-h/2}^{h/2}(m_{xx}, m_{\theta\theta}, m_{zz}, m_{x\theta}, m_{xz}, m_{z\theta})dz, \\ &(T_{xx}, T_{\theta\theta}, T_{zz}, T_{x\theta}, T_{xz}, T_{z\theta}) = \int_{-h/2}^{h/2}(m_{xx}, m_{\theta\theta}, m_{zz}, m_{x\theta}, m_{xz}, m_{z\theta})zdz \end{aligned} \quad (8)$$

The kinetic energy variation of the cylindrical shell can be expressed as:

$$\delta T = \int_X \iint_A \rho(z,T)\left\{ \begin{array}{l} (\frac{\partial u}{\partial t} + z\frac{\partial\psi_x}{\partial t})(\frac{\partial}{\partial t}\delta u + z\frac{\partial}{\partial t}\delta\psi_x) + \\ (\frac{\partial v}{\partial t} + z\frac{\partial\psi_\theta}{\partial t})(\frac{\partial}{\partial t}\delta v + z\frac{\partial}{\partial t}\delta\psi_\theta) + (\frac{\partial w}{\partial t})\frac{\partial}{\partial t}\delta w \end{array} \right\} R\,dx\,dz\;d\theta \quad (9)$$

Also the variation of work done by the surrounding elastic medium can be written as:

$$\delta W = \int_{-h/2}^{h/2}\int_0^L\int_0^{2\pi} K_w \delta w - K_p\left(\frac{\partial^2}{\partial x^2}+\frac{\partial^2}{R^2\partial\theta^2}\right)\delta w R d\theta dx dz \tag{10}$$

Substituting Eqs. (7), (9) and (10) into (6) and integrating by parts, the motion equations and boundary conditions for one layer of FG cylindrical microshell are obtained using the modified couple stress theory and first order shear deformation shell model as bellow:

For inner nanotube:

$$\begin{aligned}\delta u_1 : &\frac{\partial N^1{}_{xx}}{\partial x}+\frac{1}{R}\frac{\partial N^1{}_{x\theta}}{\partial\theta}+\frac{1}{2R^2}\left(-\frac{\partial Y^1{}_{\theta\theta}}{\partial\theta}+\frac{\partial Y^1{}_{zz}}{\partial\theta}\right)+\\ &\frac{1}{2R}\frac{\partial^2 Y^1{}_{zx}}{\partial\theta\partial x}+\frac{1}{2R^2}\frac{\partial^2 Y^1{}_{\theta z}}{\partial\theta^2}\\ &= I^1{}_0\frac{\partial^2 u_1}{\partial t^2}+I^1{}_1\frac{\partial^2\psi_{1x}}{\partial t^2}\end{aligned} \tag{11-a}$$

$$\begin{aligned}\delta v_1 : &\frac{\partial N^1{}_{x\theta}}{\partial x}+\frac{1}{R}\frac{\partial}{\partial\theta}N^1{}_{\theta\theta}+\frac{Q^1{}_{z\theta}}{R}+\\ &\frac{1}{2}\left\{\begin{array}{l}\frac{1}{R}\frac{\partial}{\partial x}\left(-Y^1{}_{xx}+Y^1{}_{\theta\theta}\right)\\ -\frac{1}{R^2}\frac{\partial Y^1{}_{\theta x}}{\partial\theta}-\frac{\partial^2 Y^1{}_{xz}}{\partial x^2}-\frac{Y^1{}_{xz}}{R^2}-\frac{1}{R}\frac{\partial^2 Y^1{}_{z\theta}}{\partial\theta\partial x}\end{array}\right\}\\ &= I^1{}_0\left[\frac{\partial^2 v_1}{\partial t^2}\right]+I^1{}_1\left\{\frac{\partial^2\psi_{1\theta}}{\partial t^2}\right\}\end{aligned} \tag{11-b}$$

$$\begin{aligned}\delta w_1 : &\frac{\partial Q^1{}_{xz}}{\partial x}+\frac{1}{R}\frac{\partial Q^1{}_{z\theta}}{\partial\theta}-\frac{N^1{}_{\theta\theta}}{R}-\frac{1}{2R^2}\frac{\partial^2 Y^1{}_{\theta x}}{\partial\theta^2}-\frac{1}{2R^2}\frac{\partial Y^1{}_{zx}}{\partial\theta}+\\ &\frac{1}{2R}\frac{\partial Y^1{}_{\theta z}}{\partial x}+\frac{\partial^2 Y^1{}_{x\theta}}{2\partial x^2}-\frac{1}{2R}\frac{\partial^2}{\partial\theta\partial x}\left(Y^1{}_{xx}-Y^1{}_{\theta\theta}\right)-K_1(w_1-w_2)+\\ &K_{1p}\nabla^2(w_1-w_2)=I^1{}_0\left(\frac{\partial^2 w_1}{\partial t^2}\right)\end{aligned} \tag{11-c}$$

$$\begin{aligned}\delta\psi_{1x} : &\frac{\partial M^1{}_{xx}}{\partial x}+\frac{1}{R}\frac{\partial M^1{}_{\theta\theta}}{\partial\theta}-Q^1{}_{xz}+\frac{1}{2}\frac{\partial Y^1{}_{\theta x}}{\partial x}-\frac{1}{2R}\frac{\partial}{\partial\theta}\left(Y^1{}_{zz}-Y^1{}_{\theta\theta}\right)+\\ &\frac{Y^1{}_{zz}}{R}+\frac{1}{2R}\frac{\partial^2 T^1{}_{zx}}{\partial\theta\partial x}+\frac{1}{2R^2}\frac{\partial^2 T^1{}_{\theta z}}{\partial\theta^2}=I^1{}_1\frac{\partial^2 u_1}{\partial t^2}+I^1{}_2\frac{\partial^2\psi_{1x}}{\partial t^2}\end{aligned} \tag{11-d}$$

$$\delta\psi_{1\theta}:\frac{1}{R}\frac{\partial M^{1}{}_{\theta\theta}}{\partial\theta}+\frac{\partial M^{1}{}_{x\theta}}{\partial x}-Q^{1}{}_{z\theta}+\frac{1}{2}\frac{\partial}{\partial x}(Y^{1}{}_{zz}-Y^{1}{}_{xx}+\frac{T^{1}{}_{\theta\theta}}{R})-\frac{1}{2}\frac{\partial Y^{1}{}_{\theta x}}{\partial\theta}+\frac{Y^{1}{}_{xz}}{2R}-\frac{1}{2R}\frac{\partial^{2}T^{1}{}_{\theta z}}{\partial\theta\partial x}-\frac{1}{2}\frac{\partial^{2}T^{1}{}_{zx}}{\partial x^{2}}=I^{1}{}_{1}\left(\frac{\partial^{2}v_{1}}{\partial t^{2}}\right)+I^{1}{}_{2}\left(\frac{\partial^{2}\psi_{1\theta}}{\partial t^{2}}\right) \tag{11-e}$$

For outer nanotube:

$$\delta u_{2}:\frac{\partial N^{2}{}_{xx}}{\partial x}+\frac{1}{R}\frac{\partial N^{2}{}_{x\theta}}{\partial\theta}+\frac{1}{2R^{2}}(-\frac{\partial Y^{2}{}_{\theta\theta}}{\partial\theta}+\frac{\partial Y^{2}{}_{zz}}{\partial\theta})+\frac{1}{2R}\frac{\partial^{2}Y^{2}{}_{zx}}{\partial\theta\partial x}+\frac{1}{2R^{2}}\frac{\partial^{2}Y^{2}{}_{\theta z}}{\partial\theta^{2}}=I^{2}{}_{0}\frac{\partial^{2}u_{2}}{\partial t^{2}}+I^{2}{}_{1}\frac{\partial^{2}\psi_{2x}}{\partial t^{2}} \tag{12-a}$$

$$\delta v_{2}:\frac{\partial N^{2}{}_{x\theta}}{\partial x}+\frac{1}{R}\frac{\partial}{\partial\theta}N^{2}{}_{\theta\theta}+\frac{Q^{2}{}_{z\theta}}{R}+\frac{1}{2}\left\{\begin{array}{l}\frac{1}{R}\frac{\partial}{\partial x}(-Y^{2}{}_{xx}+Y^{2}{}_{\theta\theta})\\-\frac{1}{R^{2}}\frac{\partial Y^{2}{}_{\theta x}}{\partial\theta}-\frac{\partial^{2}Y^{2}{}_{xz}}{\partial x^{2}}-\frac{Y^{2}{}_{xz}}{R^{2}}-\frac{1}{R}\frac{\partial^{2}Y^{2}{}_{z\theta}}{\partial\theta\partial x}\end{array}\right\}=I^{2}{}_{0}\left[\frac{\partial^{2}v_{2}}{\partial t^{2}}\right]+I^{2}{}_{1}\left\{\frac{\partial^{2}\psi_{2\theta}}{\partial t^{2}}\right\} \tag{12-b}$$

$$\delta w_{2}:\frac{\partial Q^{2}{}_{xz}}{\partial x}+\frac{1}{R}\frac{\partial Q^{2}{}_{z\theta}}{\partial\theta}-\frac{N^{2}{}_{\theta\theta}}{R}-\frac{1}{2R^{2}}\frac{\partial^{2}Y^{2}{}_{\theta x}}{\partial\theta^{2}}-\frac{1}{2R^{2}}\frac{\partial Y^{2}{}_{zx}}{\partial\theta}+\frac{1}{2R}\frac{\partial Y^{2}{}_{\theta z}}{\partial x}+\frac{\partial^{2}Y^{2}{}_{x\theta}}{2\partial x^{2}}-\frac{1}{2R}\frac{\partial^{2}}{\partial\theta\partial x}(Y^{2}{}_{xx}-Y^{2}{}_{\theta\theta})-K_{1}(w_{2}-w_{1})+K_{1p}\nabla^{2}(w_{2}-w_{1})=I^{2}{}_{0}(\frac{\partial^{2}w_{2}}{\partial t^{2}}) \tag{12-c}$$

$$\delta\psi_{2x}:\frac{\partial M^{2}_{xx}}{\partial x}+\frac{1}{R}\frac{\partial M^{2}_{\theta\theta}}{\partial\theta}-Q^{2}_{xz}+\frac{1}{2}\frac{\partial Y^{2}_{\theta x}}{\partial x}-\frac{1}{2R}\frac{\partial}{\partial\theta}(Y^{2}_{zz}-Y^{2}_{\theta\theta})+\frac{Y^{2}_{zz}}{R}+\frac{1}{2R}\frac{\partial^{2}T^{2}_{zx}}{\partial\theta\partial x}+\frac{1}{2R^{2}}\frac{\partial^{2}T^{2}_{\theta z}}{\partial\theta^{2}}=I^{2}_{1}\frac{\partial^{2}u_{2}}{\partial t^{2}}+I^{2}_{2}\frac{\partial^{2}\psi_{2x}}{\partial t^{2}} \tag{12-d}$$

$$\delta\psi_{2\theta}:\frac{1}{R}\frac{\partial M^{2}_{\theta\theta}}{\partial\theta}+\frac{\partial M^{2}_{x\theta}}{\partial x}-Q^{2}_{z\theta}+\frac{1}{2}\frac{\partial}{\partial x}(Y^{2}_{zz}-Y^{2}_{xx}+\frac{T^{2}_{\theta\theta}}{R})-\frac{1}{2}\frac{\partial Y^{2}_{\theta x}}{\partial\theta}+\frac{Y^{2}_{xz}}{2R}-\frac{1}{2R}\frac{\partial^{2}T^{2}_{\theta z}}{\partial\theta\partial x}-\frac{1}{2}\frac{\partial^{2}T^{2}_{zx}}{\partial x^{2}}=I^{2}_{1}\left(\frac{\partial^{2}v_{2}}{\partial t^{2}}\right)+I^{2}_{2}\left(\frac{\partial^{2}\psi_{2\theta}}{\partial t^{2}}\right) \tag{12-e}$$

Finally, by substituting Eq.(8) into Eqs. (11)-(12), the governing equations for each layer of the structure can be obtained. Also, associate boundary conditions for each nanotube are as below:

$$\delta u=0 \quad or$$
$$(N_{xx}+\frac{1}{4R}\frac{\partial Y_{xz}}{\partial\theta})n_{x}+(N_{x\theta}-\frac{Y_{\theta\theta}-Y_{zz}}{2R}+\frac{1}{4}\frac{\partial Y_{xz}}{\partial x}+\frac{1}{2R}\frac{\partial Y_{\theta z}}{\partial\theta})n_{\theta}=0 \tag{13-a}$$

$$\delta v=0 \quad or$$
$$(N_{x\theta}+\frac{Y_{\theta\theta}-Y_{xx}}{2R}-\frac{1}{2}\frac{\partial Y_{xz}}{\partial x}-\frac{1}{4R}\frac{\partial Y_{\theta z}}{\partial\theta})n_{x}+(N_{\theta\theta}-\frac{1}{4R}\frac{\partial Y_{\theta z}}{\partial x}-\frac{Y_{\theta x}}{2R})n_{\theta}=0 \tag{13-b}$$

$$\delta w=0 \quad or$$
$$(Q_{xz}+\frac{Y_{z\theta}}{2R}+\frac{1}{2}\frac{\partial Y_{x\theta}}{\partial x}+\frac{1}{4R}\frac{\partial(Y_{\theta\theta}-Y_{xx})}{\partial\theta})n_{x}+(Q_{\theta z}-\frac{Y_{zx}}{2R}-\frac{1}{2R}\frac{\partial Y_{x\theta}}{\partial\theta}+\frac{1}{4}\frac{\partial(Y_{\theta\theta}-Y_{xx})}{\partial x})n_{\theta}=0 \tag{13-c}$$

$$\delta\psi_x = 0 \quad or$$
$$(M_{xx} + \frac{1}{4R}\frac{\partial T_{xz}}{\partial\theta} + \frac{Y_{x\theta}}{2})n_x + \tag{13-d}$$
$$(M_{\theta x} + \frac{1}{4}\frac{\partial T_{xz}}{\partial x} + \frac{1}{2R}\frac{\partial T_{\theta z}}{\partial\theta} + \frac{(Y_{\theta\theta} - Y_{zz})}{2})n_\theta = 0$$

$$\delta\psi_\theta = 0 \quad or$$
$$(M_{x\theta} - \frac{(Y_{xx} - Y_{zz})}{2} - \frac{1}{4R}\frac{\partial T_{\theta z}}{\partial\theta} - \frac{1}{2}\frac{\partial T_{xz}}{\partial x} + \frac{T_{\theta\theta}}{2R})n_x + \tag{13-e}$$
$$(M_{\theta\theta} - \frac{Y_{x\theta}}{2} - \frac{1}{4}\frac{\partial T_{\theta z}}{\partial x})n_\theta = 0$$

For example:

The clamped boundary conditions at x=0, L:

$$u = v = w = \psi_x = \psi_\theta = 0 \tag{14}$$

The simply supported boundary conditions at x=0, L:

$$v = w = \psi_\theta = 0,$$
$$(N_{xx} + \frac{1}{4R}\frac{\partial Y_{xz}}{\partial\theta}) = 0, \quad (M_{xx} + \frac{1}{4R}\frac{\partial T_{xz}}{\partial\theta} + \frac{Y_{x\theta}}{2}) = 0. \tag{15}$$

3 Solution procedure

Generalized Differential Quadrature method (GDQ) has comprehensively used to solve the governing equations of motion in such structures, Ghadiri et al [16]. Surveying the literature reveals the shortcoming of investigations on the vibration analysis of the moderately thick cylindrical micro-shell considering the modified couple stress and centrifugal force.
In this study, GDQ method is used to calculate the spatial derivatives of field variables in equilibrium equations. In the implementation of GDQ, Grid points describe the locations of calculated derivatives and field variables. Thus, the *"r – th"* order derivative of a function *"f(x)"* can be defined as the linear summation of the function values which is:

$$\left.\frac{\partial^r f(x)}{\partial x^r}\right|_{x=x_P} = \sum_{j=1}^{n} C_{ij}^{(r)} f(x_i) \tag{16}$$

Where, n is the number of grid points along the x direction. Also, C_{ij} is obtained as follows:

$$C_{ij}^{(1)} = \begin{cases} \dfrac{M(r_i)}{(r_i - r_j)M(r_j)} & i \neq j \\ -\sum\limits_{j=1, i\neq j}^{n} C_{ij}^{(1)} & i = j \end{cases} \tag{17}$$

and M is defined as:

$$M\left(x_i\right)=\prod_{j=1,\, j\neq i}^{n}\left(x_i-x_j\right) \tag{18}$$

Superscript *"r"* is the order of the derivative. Also, $C^{(r)}$ is the weighing coefficient along the *x* direction, which could be written as:

$$C_{ij}^{(r)}=\begin{cases} r\left[C_{ij}^{(r-1)}C_{ij}^{(1)}-\dfrac{C_{ij}^{(r-1)}}{\left(r_i-r_j\right)}\right] & i\neq j \text{ and } 2\leq r\leq n-1 \\ -\displaystyle\sum_{j=1,\, i\neq j}^{n}C_{ij}^{(r)} & i=j \text{ and } 1\leq r\leq n-1 \end{cases} \tag{19}$$

In order to obtain a better mesh point distribution, Chebyshev-Gauss-Lobatto technique has been defined:

$$r_i=\frac{1}{2}\left(1-\cos\left(\frac{(i-1)}{(N-1)}\pi\right)\right) \qquad i=1,2,3,\ldots,n \tag{20}$$

The degrees of freedom of each layer of the structure can be assumed as follows:

$$\begin{aligned} u(x,\theta,t)&=U(x,\theta)e^{i\omega t},\\ v(x,\theta,t)&=V(x,\theta)e^{i\omega t},\\ w(x,\theta,t)&=W(x,\theta)e^{i\omega t},\\ \psi_x(x,\theta,t)&=\Psi_x(x,\theta)e^{i\omega t},\\ \psi_\theta(x,\theta,t)&=\Psi_\theta(x,\theta)e^{i\omega t}. \end{aligned} \tag{21}$$

Substituting Eq. (21) into the governing equations turns it into a set of algebraic equations expressed as:

δu :

$$\left\{\begin{array}{l} A_{11}\sum_{k=1}^{N_i} C_{i,k}^{(2)} + \frac{A_{55}}{R^2}\sum_{k=1}^{N_j} \bar{C}_{i,k}^{(2)} - \frac{A_{55}l^2}{4R^2}\sum_{k1=1}^{N_j}\sum_{k2=1}^{N_j} C_{i,k1}^{(2)}\bar{C}_{i,k2}^{(2)} + \\ (-\frac{A_{55}l^2}{4R^4}\sum_{k=1}^{N_j}\bar{C}_{i,k}^{(4)}) + \frac{A_{55}l^2}{R^4}\sum_{k=1}^{N_j}\bar{C}_{i,k}^{(2)} \end{array}\right\} u$$

$$+\left\{\begin{array}{l} \frac{A_{12}}{R}\sum_{k1=1}^{N_j}\sum_{k2=1}^{N_j} C_{i,k1}^{(1)}\bar{C}_{i,k2}^{(1)} + \frac{A_{55}}{R}\sum_{k1=1}^{N_j}\sum_{k2=1}^{N_j} C_{i,k1}^{(1)}\bar{C}_{i,k2}^{(1)} + \\ \frac{A_{55}l^2}{4R}\sum_{k1=1}^{N_j}\sum_{k2=1}^{N_j} C_{i,k1}^{(3)}\bar{C}_{i,k2}^{(1)} \\ +\frac{A_{55}l^2}{4R^3}(-\sum_{k1=1}^{N_j}\sum_{k2=1}^{N_j} C_{i,k1}^{(1)}\bar{C}_{i,k2}^{(1)} + v\sum_{k1=1}^{N_j}\sum_{k2=1}^{N_j} C_{i,k1}^{(1)}\bar{C}_{i,k2}^{(3)}) \end{array}\right\} v$$

$$+\left\{\frac{A_{12}}{R}\sum_{k=1}^{N_i} C_{i,k}^{(1)} + \frac{A_{55}l^2}{2R^3}\sum_{k1=1}^{N_j}\sum_{k2=1}^{N_j} C_{i,k1}^{(1)}\bar{C}_{i,k2}^{(2)}\right\} w \qquad (22)$$

$$+\left\{\begin{array}{l} B_{11}\sum_{k=1}^{N_i} C_{i,k}^{(2)} + \frac{B_{55}n^2}{R^2}\sum_{k=1}^{N_j}\bar{C}_{i,k}^{(2)} - \frac{B_{55}l^2}{4R^2}\sum_{k1=1}^{N_j}\sum_{k2=1}^{N_j} C_{i,k1}^{(2)}\bar{C}_{i,k2}^{(2)} + \\ (\frac{-5A_{55}l^2}{4R^3}\sum_{k=1}^{N_j}\bar{C}_{i,k}^{(2)} - \frac{B_{55}l^2}{4R^4}\sum_{k=1}^{N_j}\bar{C}_{i,k}^{(4)}) \end{array}\right\} \psi_x$$

$$+\left\{\begin{array}{l} \frac{B_{12}}{R}\sum_{k1=1}^{N_j}\sum_{k2=1}^{N_j} C_{i,k1}^{(1)}\bar{C}_{i,k2}^{(1)} + \frac{B_{55}}{R}\sum_{k1=1}^{N_j}\sum_{k2=1}^{N_j} C_{i,k1}^{(1)}\bar{C}_{i,k2}^{(1)} + \\ \frac{B_{55}l^2}{4R}\sum_{k1=1}^{N_j}\sum_{k2=1}^{N_j} C_{i,k1}^{(1)}\bar{C}_{i,k2}^{(3)} \\ -(\frac{B_{55}l^2}{2R^3}\sum_{k1=1}^{N_j}\sum_{k2=1}^{N_j} C_{i,k1}^{(1)}\bar{C}_{i,k2}^{(1)} + \frac{A_{55}l^2}{4R^2}\sum_{k1=1}^{N_j}\sum_{k2=1}^{N_j} C_{i,k1}^{(1)}\bar{C}_{i,k2}^{(1)} + \\ \frac{B_{55}l^2}{4R^3}\psi_{\theta_{,\theta^3 x}}) \end{array}\right\} \psi_\theta$$

δv :

$$
\begin{aligned}
&-\left\{\begin{array}{l}
-\frac{A_{12}}{R}\sum_{k1=1}^{N_j}\sum_{k2=1}^{N_j}C_{i,k1}^{(1)}\bar{C}_{i,k2}^{(1)}-\frac{A_{55}}{R}\sum_{k1=1}^{N_j}\sum_{k2=1}^{N_j}C_{i,k1}^{(1)}\bar{C}_{i,k2}^{(1)}- \\
\frac{A_{55}l^2}{4R}\sum_{k1=1}^{N_j}\sum_{k2=1}^{N_j}C_{i,k1}^{(3)}\bar{C}_{i,k2}^{(1)} \\
+\frac{A_{55}l^2}{4R^3}(\sum_{k1=1}^{N_j}\sum_{k2=1}^{N_j}C_{i,k1}^{(1)}\bar{C}_{i,k2}^{(1)}-\sum_{k1=1}^{N_j}\sum_{k2=1}^{N_j}C_{i,k1}^{(1)}\bar{C}_{i,k2}^{(3)})
\end{array}\right\}u \\
&+\left\{\begin{array}{l}
A_{55}\sum_{k=1}^{N_i}C_{i,k}^{(2)}+\frac{A_{11}}{R^2}\sum_{k=1}^{N_j}\bar{C}_{i,k}^{(2)}-\frac{k_sA_{55}}{R^2}-\frac{A_{55}l^2}{4}\sum_{k=1}^{N_i}C_{i,k}^{(4)}+ \\
\frac{A_{55}l^2}{4R^2}(2\sum_{k=1}^{N_i}C_{i,k}^{(2)}-\sum_{k1=1}^{N_j}\sum_{k2=1}^{N_j}C_{i,k1}^{(2)}\bar{C}_{i,k2}^{(2)})-\frac{A_{55}l^2}{4R^4})(1-\sum_{k=1}^{N_j}\bar{C}_{i,k}^{(2)})
\end{array}\right\}v \\
&+\left\{\begin{array}{l}
\frac{A_{11}}{R^2}\sum_{k=1}^{N_j}\bar{C}_{i,k}^{(1)}+\frac{k_sA_{55}}{R^2}\sum_{k=1}^{N_j}\bar{C}_{i,k}^{(1)}-\frac{A_{55}l^2}{4R^2}\sum_{k1=1}^{N_j}\sum_{k2=1}^{N_j}C_{i,k1}^{(2)}\bar{C}_{i,k2}^{(1)}- \\
\frac{A_{55}l^2}{4R^4}(\sum_{k=1}^{N_j}\bar{C}_{i,k}^{(3)}-\sum_{k=1}^{N_j}\bar{C}_{i,k}^{(1)})
\end{array}\right\}w \\
&+\left\{\begin{array}{l}
\frac{B_{55}}{R}\sum_{k1=1}^{N_j}\sum_{k2=1}^{N_j}C_{i,k1}^{(1)}\bar{C}_{i,k2}^{(1)}+\frac{B_{12}}{R}\sum_{k1=1}^{N_j}\sum_{k2=1}^{N_j}C_{i,k1}^{(1)}\bar{C}_{i,k2}^{(1)}+ \\
\frac{B_{55}l^2}{4R}\sum_{k1=1}^{N_j}\sum_{k2=1}^{N_j}C_{i,k1}^{(3)}\bar{C}_{i,k2}^{(1)}+\frac{A_{55}l^2}{2R^2}\sum_{k1=1}^{N_j}\sum_{k2=1}^{N_j}C_{i,k1}^{(1)}\bar{C}_{i,k2}^{(1)} \\
+\frac{B_{55}l^2}{4R^3}(\sum_{k1=1}^{N_j}\sum_{k2=1}^{N_j}C_{i,k1}^{(1)}\bar{C}_{i,k2}^{(3)}+\sum_{k1=1}^{N_j}\sum_{k2=1}^{N_j}C_{i,k1}^{(1)}\bar{C}_{i,k2}^{(1)})
\end{array}\right\}\psi_x \\
&+\left\{\begin{array}{l}
B_{55}\sum_{k=1}^{N_i}C_{i,k}^{(2)}+\frac{B_{11}}{R^2}\sum_{k=1}^{N_i}C_{i,k}^{(2)}+\frac{k_sA_{55}}{R}-\frac{B_{55}l^2}{4}\sum_{k=1}^{N_i}C_{i,k}^{(4)}+ \\
\frac{3A_{55}l^2}{4R}\sum_{k=1}^{N_i}C_{i,k}^{(2)}+\frac{B_{55}l^2}{2R}\sum_{k=1}^{N_i}C_{i,k}^{(2)} \\
+\frac{B_{55}l^2}{4R^2}(-\sum_{k1=1}^{N_j}\sum_{k2=1}^{N_j}C_{i,k1}^{(2)}\bar{C}_{i,k2}^{(2)}-\sum_{k=1}^{N_i}C_{i,k}^{(2)})+\frac{A_{55}l^2}{4R^3}(1+\sum_{k=1}^{N_j}\bar{C}_{i,k}^{(2)})
\end{array}\right\}\psi_\theta
\end{aligned}
\tag{23}
$$

δw :

$$
\begin{aligned}
&-\left\{\frac{A_{12}}{R}\sum_{k=1}^{N_i}C_{i,k}^{(1)}+\frac{A_{55}l^2}{2R^3}\sum_{k1=1}^{N_j}\sum_{k2=1}^{N_j}C_{i,k1}^{(1)}\bar{C}_{i,k2}^{(2)}\right\}u\\
&+\left\{\begin{array}{l}-\frac{A_{11}}{R^2}\sum_{k=1}^{N_j}\bar{C}_{i,k}^{(1)}-\frac{k_sA_{55}}{R^2}\sum_{k=1}^{N_j}\bar{C}_{i,k}^{(1)}+\frac{A_{55}l^2}{4R^2}\sum_{k1=1}^{N_j}\sum_{k2=1}^{N_j}C_{i,k1}^{(2)}\bar{C}_{i,k2}^{(1)}\\-\frac{A_{55}l^2}{4R^4}(-\sum_{k=1}^{N_j}\bar{C}_{i,k}^{(3)}+\sum_{k=1}^{N_j}\bar{C}_{i,k}^{(1)})\end{array}\right\}v\\
&+\left\{\begin{array}{l}k_sA_{55}\sum_{k=1}^{N_i}C_{i,k}^{(2)}+\frac{k_sA_{55}}{R^2}\sum_{k=1}^{N_j}\bar{C}_{i,k}^{(2)}-\frac{A_{11}}{R^2}-\frac{A_{55}l^2}{4}\sum_{k=1}^{N_i}C_{i,k}^{(2)}\\+\frac{A_{55}l^2}{4R^2}(-2\sum_{k1=1}^{N_j}\sum_{k2=1}^{N_j}C_{i,k1}^{(2)}\bar{C}_{i,k2}^{(2)}+\sum_{k=1}^{N_i}C_{i,k}^{(2)})-\\\frac{A_{55}l^2}{4R^4}(-\sum_{k=1}^{N_j}\bar{C}_{i,k}^{(2)}+\sum_{k=1}^{N_j}\bar{C}_{i,k}^{(4)})\end{array}\right\}w\\
&+\left\{\begin{array}{l}k_sA_{55}\sum_{k=1}^{N_i}C_{i,k}^{(1)}-\frac{B_{12}}{R}\sum_{k=1}^{N_i}C_{i,k}^{(1)}+\frac{A_{55}l^2}{4}\sum_{k=1}^{N_i}C_{i,k}^{(3)}-\\\frac{A_{55}l^2}{4R^2}(-\sum_{k1=1}^{N_j}\sum_{k2=1}^{N_j}C_{i,k1}^{(1)}\bar{C}_{i,k2}^{(2)}+\sum_{k=1}^{N_i}C_{i,k}^{(1)})\end{array}\right\}\psi_x\\
&+\left\{\begin{array}{l}\frac{k_sA_{55}}{R}\sum_{k=1}^{N_j}\bar{C}_{i,k}^{(1)}-\frac{B_{11}}{R^2}\sum_{k=1}^{N_j}\bar{C}_{i,k}^{(1)}+\frac{B_{55}l^2\sum_{k1=1}^{N_j}\sum_{k2=1}^{N_j}C_{i,k1}^{(2)}\bar{C}_{i,k2}^{(1)}}{2R^2}-\\\frac{A_{55}l^2\sum_{k1=1}^{N_j}\sum_{k2=1}^{N_j}C_{i,k1}^{(2)}\bar{C}_{i,k2}^{(1)}}{4R}\\+\frac{A_{55}l^2}{4R^3}(\sum_{k=1}^{N_j}\bar{C}_{i,k}^{(1)}+\sum_{k=1}^{N_j}\bar{C}_{i,k}^{(3)})\end{array}\right\}\psi_\theta
\end{aligned}
\tag{24}
$$

$\delta\psi_x$:

$$
\begin{Bmatrix}
+B_{11}\sum_{k=1}^{N_i} C_{i,k}^{(2)} + \frac{B_{55}}{R^2}\sum_{k=1}^{N_j} \bar{C}_{i,k}^{(2)} - \frac{B_{55}l^2}{4R^2}\sum_{k1=1}^{N_j}\sum_{k2=1}^{N_j} C_{i,k1}^{(2)}\bar{C}_{i,k2}^{(2)} - \\
(\frac{5A_{55}l^2}{4R^3}\sum_{k=1}^{N_j} \bar{C}_{i,k}^{(2)} + \frac{B_{55}l^2n^4}{4R^4}\sum_{k=1}^{N_j} \bar{C}_{i,k}^{(4)})
\end{Bmatrix} u
$$

$$
-\begin{Bmatrix}
-\frac{B_{55}}{R}\sum_{k1=1}^{N_j}\sum_{k2=1}^{N_j} C_{i,k1}^{(1)}\bar{C}_{i,k2}^{(1)} - \frac{B_{12}}{R}\sum_{k1=1}^{N_j}\sum_{k2=1}^{N_j} C_{i,k1}^{(1)}\bar{C}_{i,k2}^{(1)} - \\
\frac{B_{55}l^2}{4R}\sum_{k1=1}^{N_j}\sum_{k2=1}^{N_j} C_{i,k1}^{(3)}\bar{C}_{i,k2}^{(1)} - (\frac{A_{55}l^2}{2R^2}\sum_{k1=1}^{N_j}\sum_{k2=1}^{N_j} C_{i,k1}^{(1)}\bar{C}_{i,k2}^{(1)} + \\
\frac{B_{55}l^2(\sum_{k1=1}^{N_j}\sum_{k2=1}^{N_j} C_{i,k1}^{(1)}\bar{C}_{i,k2}^{(3)} + \sum_{k1=1}^{N_j}\sum_{k2=1}^{N_j} C_{i,k1}^{(1)}\bar{C}_{i,k2}^{(1)})}{4R^3})
\end{Bmatrix} v
$$

$$
-\begin{Bmatrix}
k_s A_{55}\sum_{k=1}^{N_i} C_{i,k}^{(1)} - \frac{B_{12}}{R}\sum_{k=1}^{N_i} C_{i,k}^{(1)} + \frac{A_{77}l^2}{4}\sum_{k=1}^{N_i} C_{i,k}^{(3)} - \\
\frac{A_{55}l^2(-\sum_{k1=1}^{N_j}\sum_{k2=1}^{N_j} C_{i,k1}^{(1)}\bar{C}_{i,k2}^{(2)} + \sum_{k=1}^{N_i} C_{i,k}^{(1)})}{4R^2})
\end{Bmatrix} w \qquad (25)
$$

$$
+\begin{Bmatrix}
D_{11}\sum_{k=1}^{N_i} C_{i,k}^{(2)} + \frac{D_{55}}{R^2}\sum_{k=1}^{N_j} \bar{C}_{i,k}^{(2)} - k_s A_{55} + \\
(-\frac{D_{55}l^2}{4R^4}\sum_{k=1}^{N_j} \bar{C}_{i,k}^{(4)} - \frac{2B_{55}l^2}{4R^3}\sum_{k=1}^{N_j} \bar{C}_{i,k}^{(4)} \\
-\frac{A_{55}l^2(1-4\sum_{k=1}^{N_j} \bar{C}_{i,k}^{(2)})}{4R^2}) - \frac{D_{55}l^2}{4R^2}\sum_{k1=1}^{N_j}\sum_{k2=1}^{N_j} C_{i,k1}^{(2)}\bar{C}_{i,k2}^{(2)} + \frac{A_{55}l^2}{4}\sum_{k=1}^{N_i} C_{i,k}^{(2)}
\end{Bmatrix} \psi_x
$$

$$
+\begin{Bmatrix}
\frac{D_{12}}{R}\sum_{k1=1}^{N_j}\sum_{k2=1}^{N_j} C_{i,k1}^{(1)}\bar{C}_{i,k2}^{(1)} + \frac{D_{55}}{R}\sum_{k1=1}^{N_j}\sum_{k2=1}^{N_j} C_{i,k1}^{(1)}\bar{C}_{i,k2}^{(1)} + \\
\frac{D_{55}l^2}{4R}\sum_{k1=1}^{N_j}\sum_{k2=1}^{N_j} C_{i,k1}^{(3)}\bar{C}_{i,k2}^{(1)} + \frac{D_{55}l^2}{4R^3}\sum_{k1=1}^{N_j}\sum_{k2=1}^{N_j} C_{i,k1}^{(1)}\bar{C}_{i,k2}^{(3)} + \\
\frac{B_{55}l^2}{2R}\sum_{k1=1}^{N_j}\sum_{k2=1}^{N_j} C_{i,k1}^{(1)}\bar{C}_{i,k2}^{(1)} - \frac{3A_{55}l^2}{4R}\sum_{k1=1}^{N_j}\sum_{k2=1}^{N_j} C_{i,k1}^{(1)}\bar{C}_{i,k2}^{(1)}
\end{Bmatrix} \psi_\theta
$$

$\delta\psi_\theta$:

$$
\begin{Bmatrix}
-\frac{B_{12}}{R}\sum_{k1=1}^{N_j}\sum_{k2=1}^{N_j}C_{i,k1}^{(1)}\bar{C}_{i,k2}^{(1)}-\frac{B_{55}}{R}\sum_{k1=1}^{N_j}\sum_{k2=1}^{N_j}C_{i,k1}^{(1)}\bar{C}_{i,k2}^{(1)}- \\
\frac{B_{55}l^2}{4R}\sum_{k1=1}^{N_j}\sum_{k2=1}^{N_j}C_{i,k1}^{(3)}\bar{C}_{i,k2}^{(1)}+\frac{B_{55}l^2}{2R^3}\sum_{k1=1}^{N_j}\sum_{k2=1}^{N_j}C_{i,k1}^{(1)}\bar{C}_{i,k2}^{(1)}+ \\
\frac{A_{55}l^2}{4R^2}\sum_{k1=1}^{N_j}\sum_{k2=1}^{N_j}C_{i,k1}^{(1)}\bar{C}_{i,k2}^{(1)}+\frac{B_{55}l^2n^3}{4R^3}\sum_{k1=1}^{N_j}\sum_{k2=1}^{N_j}C_{i,k1}^{(1)}\bar{C}_{i,k2}^{(3)}
\end{Bmatrix}u
$$

$$
+\begin{Bmatrix}
B_{55}v_{,x^2}+\frac{B_{11}}{R^2}\sum_{k=1}^{N_j}\bar{C}_{i,k}^{(2)}+\frac{k_sA_{55}}{R}-\frac{B_{55}l^2}{4}\sum_{k=1}^{N_i}C_{i,k}^{(4)} \\
-(\frac{-3A_{55}l^2}{4R}\sum_{k=1}^{N_i}C_{i,k}^{(2)}-\frac{B_{55}l^2}{2R}\sum_{k=1}^{N_i}C_{i,k}^{(2)}+ \\
\frac{B_{55}l^2(\sum_{k1=1}^{N_j}\sum_{k2=1}^{N_j}C_{i,k1}^{(2)}\bar{C}_{i,k2}^{(2)}+\sum_{k=1}^{N_i}C_{i,k}^{(2)})}{4R^2})+(\frac{A_{55}l^2(1+\sum_{k=1}^{N_j}\bar{C}_{i,k}^{(2)})}{4R^3})
\end{Bmatrix}v
$$

$$
+\begin{Bmatrix}
\frac{-k_sA_{55}}{R}\sum_{k=1}^{N_j}\bar{C}_{i,k}^{(1)}+\frac{B_{11}}{R^2}\sum_{k=1}^{N_j}\bar{C}_{i,k}^{(1)}+(\frac{-B_{55}l^2}{2R^2}+\frac{A_{55}l^2}{4R})\sum_{k1=1}^{N_j}\sum_{k2=1}^{N_j}C_{i,k1}^{(2)}\bar{C}_{i,k2}^{(1)} \\
-\frac{A_{77}l^2}{4R^3}(\sum_{k=1}^{N_j}\bar{C}_{i,k}^{(1)}+\sum_{k=1}^{N_j}\bar{C}_{i,k}^{(3)})
\end{Bmatrix}w \qquad (26)
$$

$$
-\begin{Bmatrix}
-\frac{D_{12}}{R}\sum_{k1=1}^{N_j}\sum_{k2=1}^{N_j}C_{i,k1}^{(1)}\bar{C}_{i,k2}^{(1)}-\frac{D_{55}}{R}\sum_{k1=1}^{N_j}\sum_{k2=1}^{N_j}C_{i,k1}^{(1)}\bar{C}_{i,k2}^{(1)}- \\
\frac{D_{55}l^2}{4R}\sum_{k1=1}^{N_j}\sum_{k2=1}^{N_j}C_{i,k1}^{(3)}\bar{C}_{i,k2}^{(1)}-\frac{D_{55}l^2}{4R^3}\sum_{k1=1}^{N_j}\sum_{k2=1}^{N_j}C_{i,k1}^{(1)}\bar{C}_{i,k2}^{(3)}- \\
\frac{B_{55}l^2}{2R}\sum_{k1=1}^{N_j}\sum_{k2=1}^{N_j}C_{i,k1}^{(1)}\bar{C}_{i,k2}^{(1)}+\frac{3A_{55}l^2}{4R}\sum_{k1=1}^{N_j}\sum_{k2=1}^{N_j}C_{i,k1}^{(1)}\bar{C}_{i,k2}^{(1)}
\end{Bmatrix}\psi_x
$$

$$
+\begin{Bmatrix}
\frac{D_{11}}{R^2}\sum_{k1=1}^{N_j}\sum_{k2=1}^{N_j}C_{i,k1}^{(1)}\bar{C}_{i,k2}^{(2)}+D_{55}\sum_{k=1}^{N_i}C_{i,k}^{(2)}-k_sA_{55}- \\
\frac{D_{55}l^2}{4}\sum_{k=1}^{N_i}C_{i,k}^{(4)}-\frac{D_{55}l^2}{4R^2}\sum_{k1=1}^{N_j}\sum_{k2=1}^{N_j}C_{i,k1}^{(2)}\bar{C}_{i,k2}^{(2)}+\frac{B_{55}l^2}{2R}\sum_{k=1}^{N_i}C_{i,k}^{(2)}+ \\
A_{55}l^2\sum_{k=1}^{N_i}C_{i,k}^{(2)}+\frac{D_{55}l^2}{2R}\sum_{k=1}^{N_i}C_{i,k}^{(2)}+\frac{A_{55}l^2n^2}{4R^2}\sum_{k=1}^{N_j}\bar{C}_{i,k}^{(2)}
\end{Bmatrix}\psi_\theta
$$

Applying GDQ method into the motion equations of the double cylindrical FG micro-shell i.e. Eqs. (10), the solution of the proposed eigenvalue equations in the form of Eq. (27) would lead to the natural frequencies where the extracted components of [M] and [K] are present.

$$[M]\omega^2 + [K] = 0 \tag{27}$$

4 Results

The numerical results of the vibration behavior of double layer cylindrical FG microshell are investigated based on the MCST for the various boundary conditions. Sufficient number of grid points is necessary to achieve accurate results in GDQ method. As it is shown in Table (1), for the good results, 31 grid points are appropriate. The Results are shown and analyzed in two sections. The first one verifies proposed model with existing literatures. Second section shows the effect of length, thickness, FG power index, Winkler and Pasternak coefficient and shear correction factor on the natural frequencies of double cylindrical FG microshell.

Table 1 The effect of the number of grid points on evaluating convergence of the natural frequency(GHz) of the double FG cylindrical microshell with respect to the different FG power index, boundary conditions (B.Cs) and L_1=L_2=10μm, L_1/R_1=10, h_1=h_2=R_1/10, l_{1m}=14μm, l_{1c}=l_{1m}/2, l_{1m}=l_{2m}, l_{1c}=l_{2c}, K_w=1e14, K_p=0, R_2=1.125× R_1

B.Cs	FG power index (m)	**N=15**	**N=19**	**N=23**	**N=27**	**N=31**	**N=34**
S-S S-S	Only metal	0.48146166	0.48146166	0.48146166	0.48146166	0.48146166	0.48146166
	1	0.68933699	0.68933699	0.68933699	0.68933699	0.68933699	0.68933699
	10	0.80166448	0.80166448	0.80166448	0.80166448	0.80166448	0.80166448
	Only ceramic	0.82412107	0.82412107	0.82412107	0.82412107	0.82412107	0.82412107
C-S C-S	Only metal	0.56806511	0.56794809	0.56794649	0.56794853	0.56794852	0.56794852
	1	0.87162888	0.87146831	0.87144774	0.87145249	0.87145264	0.87145264
	10	1.03504190	1.03490931	1.03489181	1.03489577	1.03489582	1.03489582
	Only ceramic	1.06745638	1.06732910	1.06731387	1.06731751	1.06731752	1.06731752
C-C C-C	Only metal	0.66162622	0.66164744	0.66164278	0.66164272	0.66164274	0.66164274
	1	1.06307791	1.06314833	1.06313858	1.06313795	1.06313800	1.06313800
	10	1.27890989	1.27897364	1.27896266	1.27896217	1.27896221	1.27896221
	Only ceramic	1.32155387	1.32161012	1.32159908	1.32159869	1.32159873	1.32159873

4.1 Results verification with other articles

Table (2) is presented to show the agreement of present results with those reported by other scholars with different theories. Effects of changing the thickness to radius ratio (h/R) and FG power index are observable.

Table 2 Comparison of the fundamental natural frequency (Hz) of one layer cylindrical FG shell structure for different cylindrical shell theory against h/R ratios with (L/R=20)

	h/R	m=0	m=0.5	m=0.7	m=1	m=2	m=5	m=15
Classical theory[18]	0.020	13.552	13.325	13.273	13.215	13.107	13.001	12.936
	0.030	13.557	13.330	13.278	13.220	13.112	13.006	12.941
	0.040	13.563	13.336	13.284	13.226	13.119	13.013	12.948
	0.050	13.572	13.345	13.293	13.235	13.127	13.021	12.956
Higher-order deformation theory [19]	0.020	13.4172	13.1924	13.1405	13.0828	12.9758	12.8710	12.8065
	0.030	13.4220	13.1971	13.1451	13.0874	12.9804	12.8756	12.8111
	0.040	13.4287	13.2037	13.1517	13.0939	12.9869	12.8820	12.8175
	0.050	13.4373	13.2121	13.1601	13.1023	12.9952	12.8903	12.8257
First order shear deformation theory (**Present)**	0.020	13.5156	13.2894	13.2375	13.1797	13.0722	12.9668	12.9019
	0.030	13.5204	13.2941	13.2422	13.1845	13.0769	12.9715	12.9065
	0.040	13.5271	13.3008	13.2489	13.1911	13.0835	12.9780	12.9130
	0.050	13.5356	13.3093	13.2574	13.1995	13.0919	12.9863	12.9212

With increasing the power index, the natural frequency enhances in all thicknesses; increasing the thickness leads to increase in frequency as well. Note that, all results of this table are related to natural frequency (Hz) of a simply supported cylindrical FG shell.
Another validation has been done by Ghadiri and safarpour [18]. As Fig. (1) demonstrates, there is a good accuracy in obtained natural frequencies of the FG microshell especially with increasing the length.

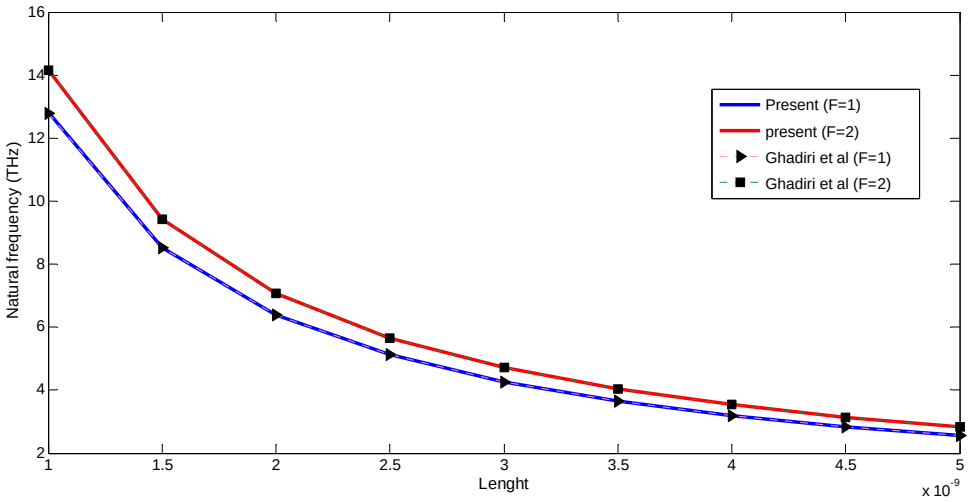

Figure 1 Comparison of the natural frequency of FG cylindrical shell with the results obtained by Ghadiri et al.[18]

4.2 Parametric results

The material for inner and outer cylindrical microshell is FGM. It is assumed that the inner surface is ceramic and the outer one is metal. Volume fraction index (m) determines the variation profile of the material properties across the thickness of the FG cylindrical microshell. The material properties are given in Table (3) as below:

Table (4) shows the effect of shear correction factor, thickness, Winkler and Pasternak stiffness coefficient on natural frequency under the various boundary conditions. As it can be seen from Table (4), an increase in shear correction factor leads to an increase in the natural frequency. This trend is observed under all types of boundary conditions. In addition, the increase in the Winkler and Pasternak stiffness coefficients results in considerable increase in natural frequency. Simply-Simply boundary condition has the lowest frequency because of its particular condition, and Clamp-Clamp boundary condition has the highest frequency. In addition, the effect of Pasternak stiffness coefficient (K_p) has remarkable effect on the natural frequency in comparison with the Winkler stiffness coefficient.

Also, by increasing the thickness, the natural frequency tends to decrease.

Table 3 Material properties of FGM constituents [16].

Material properties	Unit	Aluminum	Silicon
E	GPA	70	210
ρ	Kg/m^3	2700	2370
υ	–	0.3	0.24

Table 4 Variation of the fundamental natural frequency, with different thickness of a double layer FG cylindrical microshell for different shear correction factor, winker and Pasternak stiffness with various boundary conditions and L_1=L_2=10μm, L_1/R_1=10, h_1=h_2, l_{1m}=14μm, l_{1c}=l_{1m}/2, l_{1m}=l_{2m}, l_{1c}=l_{2c}, R_2=1.125× R_1, m=1

B.Cs	K_p=0				K_p=100			
	Ks=0		*Ks=5/6*		*Ks=0*		*Ks=5/6*	
S_S	K_w= *1e14*	K_w= *1e15*	K_w= *1e14*	K_w= *1e15*	K_w= *1e14*	K_w= *1e15*	K_w= *1e14*	K_w= *1e15*
$h_1(\mu m)$								
0.1	0.687427	1.19883	0.689337	1.20122	0.778507	1.24393	0.780368	1.24645
0.2	0.636747	0.961331	0.641959	0.965259	0.692019	0.990906	0.696887	0.994775
0.3	0.617666	0.863184	0.628401	0.871239	0.657995	0.886043	0.668113	0.893923
S_C								
$h_1(\mu m)$								
0.1	0.866874	1.331686	0.871628	1.336483	0.947203	1.374034	1.378875	0.951737
0.2	0.8242185	1.112314	0.833975	1.120407	0.871081	1.139584	1.147561	0.880383
0.3	0.8086962	1.022929	0.825464	1.036825	0.842069	1.043792	1.057477	0.858198
C_C								
$h_1(\ (\mu m)$								
0.1	1.055548	1.484719	1.063078	1.492008	1.12715	1.524666	1.134418	1.531971
0.2	1.018709	1.279139	1.034333	1.292736	1.059203	1.30451	1.074339	1.317973
0.3	1.005598	1.196397	1.031063	1.218672	1.03397	1.215613	1.058798	1.237657

It can be seen from Figs. (2)-(4) that the increase in length leads to the increase in natural frequency. Figs. (3)-(5) show the effect of the length on natural frequency (GHz) of double cylindrical FG microshell with different boundary conditions and R_1=1μm, h_1=h_2=R_1/10, l_{1m}=14μm, l_{1c}=l_{1m}/2, l_{1m}=l_{2m}, l_{1c}=l_{2c}, K_w=1e14, K_p=100, R_2=1.125× R_1.

This is because increasing the length is eventuated to decrease in stiffness and natural frequency of the double FG cylindrical microshell. Other results are that, the double cylindrical microshell which, is made of only metal, has the lower frequency in comparison with that one which is made of only ceramic. The other remarkable point is related to Fig.(3) where the effect of length on natural frequency of simply-simply boundary condition is less than two others.

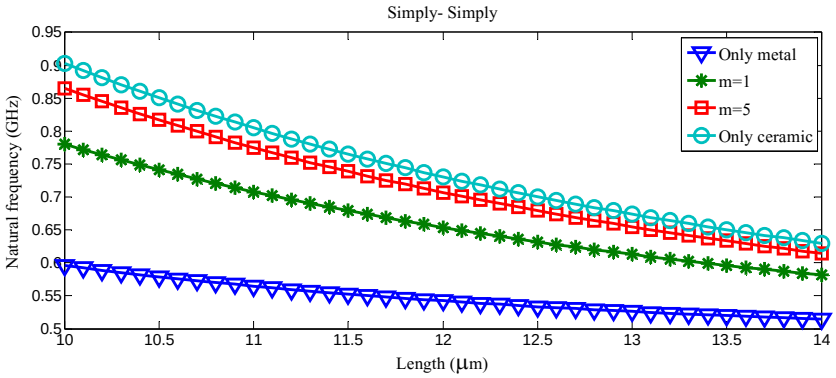

Figure 2 The effect of length on the natural frequency with simply-simply boundary condition

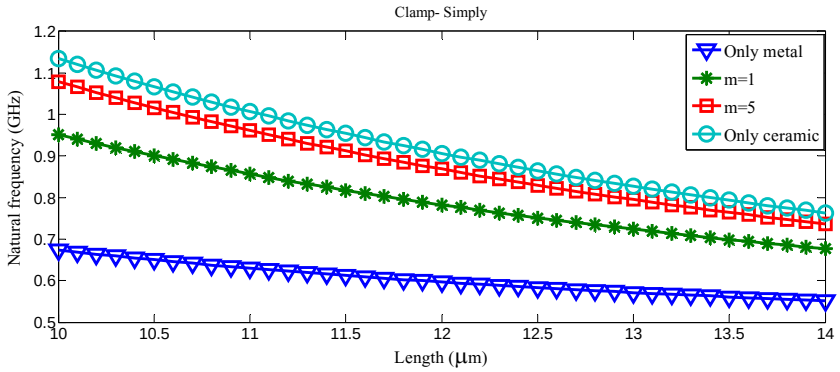

Figure 3 The effect of length on the natural frequency with clamp-simply boundary condition

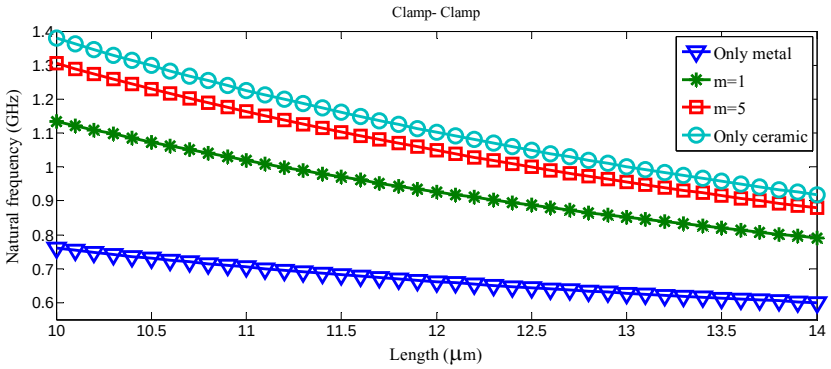

Figure 4 The effect of length on the natural frequency with clamp-clamp boundary condition

Figs. (6)-(8) illustrate the effect of Winkler foundation on natural frequency of double cylindrical microshell for the case where L_1=L_2=10μm, L_1/R_1=10, h_1=h_2=R_1/10, l_{1m}=14μm, l_{1c}=l_{1m}/2, l_{1m}=l_{2m}, l_{1c}=l_{2c}, K_p=100, R_2=1.125× R_1. Figures (6-8) respectively are related to the simply-simply, clamped-simply and clamp-clamp boundary conditions. As one can see in all three figures, with increase in Winkler stiffness coefficient, natural frequencies increase. Also increase in FG power index leads to increase in natural frequencies. In simply-simply boundary condition, frequency variations are modest again. Figs. (5)-(7) show that with considering the coefficient of Pasternak, there is an exceptional trend by increasing Winkler coefficient, at first frequency increase and reach to a peak point then the natural frequency tends to be constant in all boundary conditions.

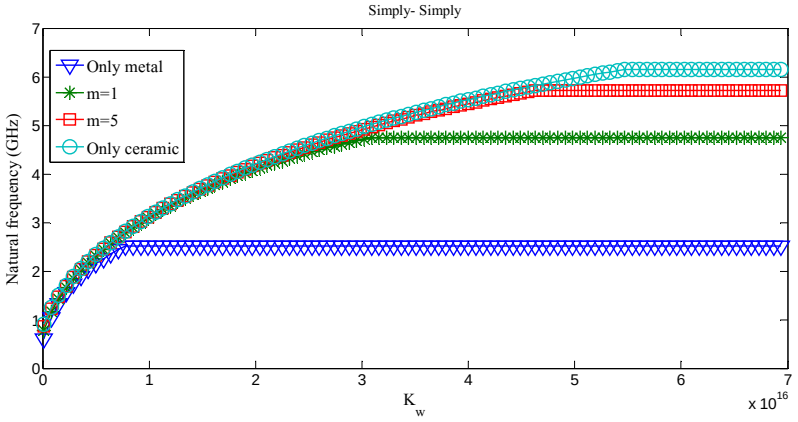

Figure 5 The effect of Winkler stiffness coefficient on the natural frequency with simply-simply boundary condition

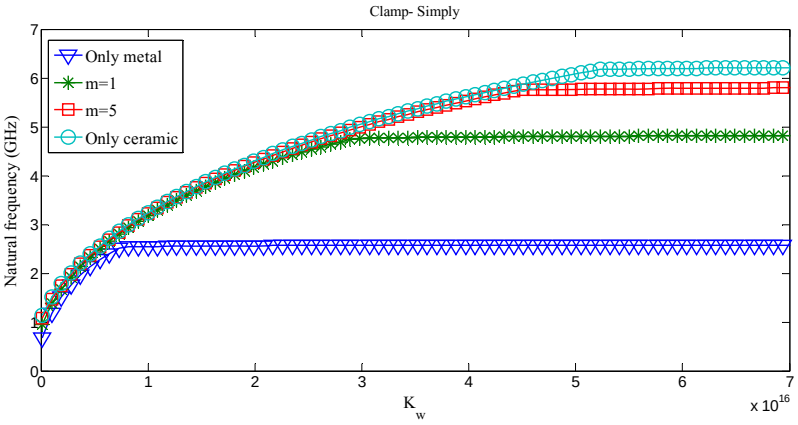

Figure 6 The effect of Winkler stiffness coefficient on the natural frequency with clamp-simply boundary condition

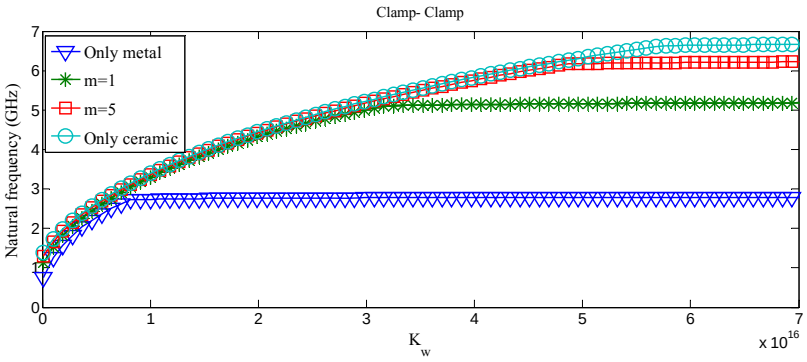

Figure 7 The effect of Winkler stiffness coefficient on the natural frequency with clamp-clamp boundary condition

Figs. (8)-(10) illustrate the effect of Pasternak foundation on natural frequency with L_1=L_2=10μm, L_1/R_1=10, h_1=h_2=R_1/10, l_{1m}=14μm, l_{1c}=l_{1m}/2, l_{1m}=l_{2m}, l_{1c}=l_{2c}, K_w=1e14, R_2=1.125× R_1. Figures (8)-(10) respectively are related to simply-simply, clamped-simply and clamp-clamp boundary conditions; as it is obvious in all figures with increase in Pasternak stiffness coefficient the natural frequencies tend to increase.

Also increase in FG power index causes to increase in natural frequencies. Also this kind of foundation has more influence on frequency in comparison with Winkler. In simply-simply boundary condition, frequency variations are modest again. Figs. (8)-(10) show that with considering the coefficient of Winkler, there is an exceptional trend by increasing pasternak coefficient, at first frequency increase and reach to a peak point then the natural frequency tends to be constant in all boundary conditions.

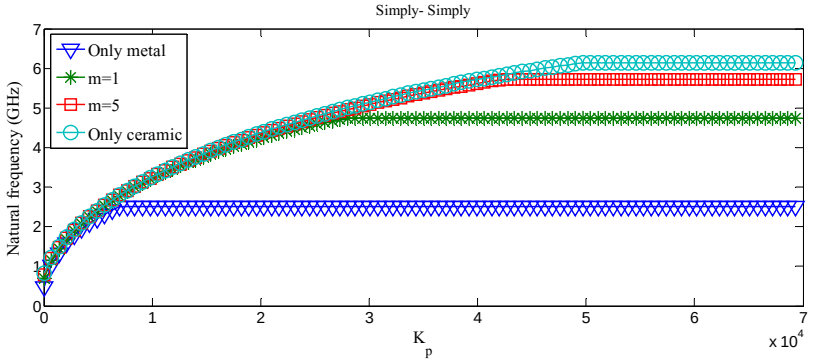

Figure 8 The effect of Pasternak stiffness coefficient on the natural frequency with simply-simply boundary condition

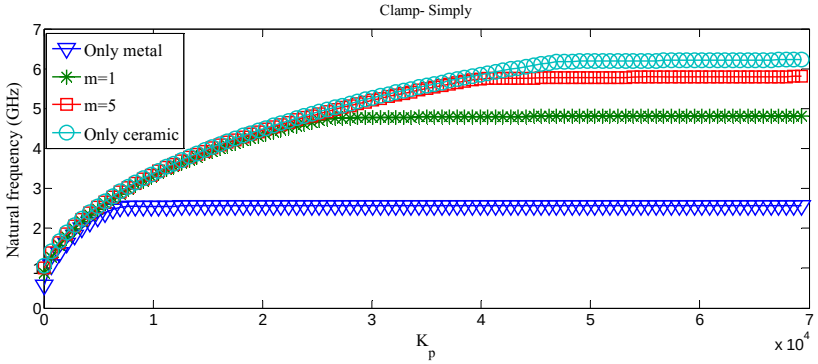

Figure 9 The effect of Pasternak stiffness on the natural frequency with clamp-simply boundary condition

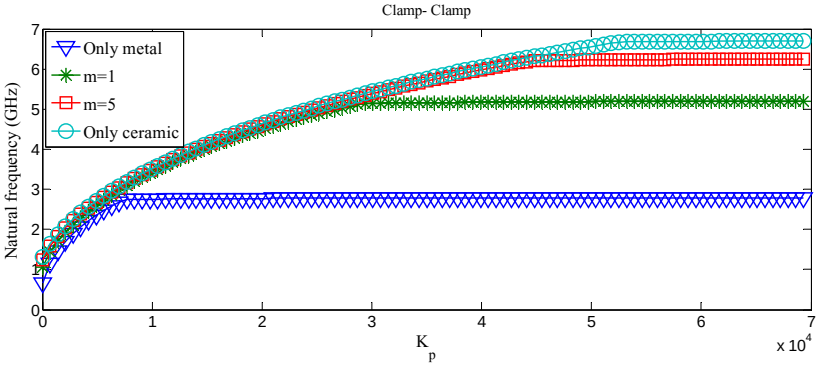

Figure 10 The effect of Pasternak stiffness coefficient on the natural frequency with clamp-clamp boundary condition

5 Conclusion

This paper presents the free vibration analysis of double layer cylindrical microshell surrounded by elastic foundation, with the inner and the outer layers made of a functionally graded material. Modified couple stress theory introduces the size-dependent effect. The equations of motion and non-classic boundary conditions are derived using Hamilton's principle. The natural frequency of the double layer cylindrical FG microshell are investigated with respect to the length, thickness, FG power index, Winkler and Pasternak coefficient and shear correction factor for different boundary conditions of the double layer cylindrical FG microshell. The following important results can be obtained from this study:

1- By increasing the length and thickness the natural frequency tends to decrease while, by increasing the FG power index, the natural frequency increases.
2- Simply-simply boundary condition has the lowest natural frequency because of its particular condition, and Clamp-Clamp boundary condition has the highest natural frequency.
3- The results show that, increase in the length to radius ratio and material length scale parameter lead to increase in the critical speed of the rotation FG cylindrical microshell.
4- By considering the coefficient of Winkler and Pasternak, there is an exceptional trend by increasing Winkler and Pasternak coefficient, at first frequency increase and reach to a peak point then the natural frequency tends to be constant in all boundary conditions.

References

[1] Haddadpour, H., Mahmoudkhani, S., and Navazi, H., "Free Vibration Analysis of Functionally Graded Cylindrical Shells Including Thermal Effects", Thin-Walled Structures, Vol. 45, pp. 591-599, (2007)

[2] Farid, M., Zahedinejad, P., and Malekzadeh, P., "Three-dimensional Temperature Dependent Free Vibration Analysis of Functionally Graded Material Curved Panels Resting on Two-parameter Elastic Foundation using a Hybrid Semi-analytic, Differential Quadrature Method", Materials & Design, Vol. 31, pp. 2-13, (2010).

[3] Rahaeifard, M., Kahrobaiyan, M., and Ahmadian, M., "Sensitivity Analysis of Atomic Force Microscope Cantilever made of Functionally Graded Materials", in ASME 2009 International Design Engineering Technical Conferences and Computers and Information in Engineering Conference, pp. 539-544, San Diego, California, USA, (2009).

[4] Lee, Z., Ophus, C., Fischer, L.M., Nelson-Fitzpatrick, N., Westra, K.L., Evoy, S., Radmilovic, V., Dahmen, U., and Mitlin, D.,"Metallic NEMS Components Fabricated from Nanocomposite Al–Mo Films", Nanotechnology, Vol. 17, pp. 3063, (2006).

[5] Ghasemabadian, M.A., and Kadkhodayan, M., "Investigation of Buckling Behavior of Functionally Graded Piezoelectric (FGP) Rectangular Plates under Open and Closed Circuit Conditions", Structural Engineering and Mechanics,Vol. 60, No. 2, pp. 271-299, (2016).

[6] Koiter, W., "*Couple Stresses in the Theory of Elasticity*," Proc. Koninklijke Nederl. Akaad. Van Wetensch, Vol. 67, (1964).

[7] Mindlin, R. D., "Micro-structure in Linear Elasticity", Archive for Rational Mechanics and Analysis, Vol. 16, pp. 51-78, (1964).

[8] Asghari, M., Kahrobaiyan, M., Rahaeifard, M., and Ahmadian, M., "Investigation of the Size Effects in Timoshenko Beams Based on the Couple Stress Theory", Archive of Applied Mechanics, Vol. 81, pp. 863-874, (2011).

[9] Yang, F., Chong, A.C.M., Lam, D.C.C., and Penger, T., "Couple Stress Based Strain Gradient Theory for Elasticity", International Journal of Solids and Structures, Vol. 39, pp. 2731-2743, (2002).

[10] Shaat, M., Mahmoud F.F., Gao, X.L., and Faheem A., " Size-dependent Bending Analysis of Kirchhoff Nano-plates Based on a Modified Couple-stress Theory Including Surface Effects", International Journal of Mechanical Sciences, Vol. 79, pp. 31-37, (2014).

[11] Miandoab, E. M., Pishkenari, H. N., Yousefi-Koma, A., and Hoorzad, H., "Polysilicon Nano-beam Model Based on Modified Couple Stress and Eringen's Nonlocal Elasticity Theories", Physica E: Low-dimensional Systems and Nanostructures, Vol. 63, pp. 223-228, (2014).

[12] Karami, H., and Farid, M., "A New Formulation to Study In-plane Vibration of Curved Carbon Nanotubes Conveying Viscous Fluid", Journal of Vibration and Control, Vol. 21, pp. 2360-2371, (2015).

[13] Choi, J., Song, O., and Kim, S. k., "Nonlinear Stability Characteristics of Carbon Nanotubes Conveying Fuids", Acta Mechanica, Vol. 224, pp. 1383-1396, (2013).

[14] Chang, T. P., "Axial Vibration of Non-uniform and Non-homogeneous Nanorods Based on Nonlocal Elasticity Theory", Applied Mathematics and Computation, Vol. 219, pp. 4933-4941, (2013).

[15] Zhang, H., Deng, Q.T., and Li, S.H., "Vibration of a Single-walled Carbon Nanotube Embedded in an Elastic Medium under a Moving Internal Nanoparticle", Applied Mathematical Modelling, Vol. 37, Issues. 10–11, pp. 6940-6951, (2013).

[16] Ghadiri, M., and Shafiei, N., "Nonlinear Bending Vibration of a Rotating Nanobeam Based on Nonlocal Eringen's Theory using Differential Quadrature Method", Microsystem Technologies, pp. 1-15, (2015).

[17] Habibi, M., Taghdir, A., and Safarpour, H., "Stability Analysis of an Electrically Cylindrical Nanoshell Reinforced with Graphene Nanoplatelets", Composites Part B: Engineering, Vol. 175, pp. 107-125, (2019).

[18] Ghadiri, M., and Safarpour, H., "Free Vibration Analysis of Embedded Magneto-electro-thermo-elastic Cylindrical Nanoshell Based on the Modified Couple Stress Theory", Applied Physics A, Vol. 122, pp. 833, (2016).

Nomenclature

E	Bulk elastic modulus
ρ	Mass density
u	Components of displacement vector
φ	Components of infinitesimal rotation vector
T	Kinetic energy of the cylinderical shell
K_P	Pasternak coefficient
K_W	Winkler coefficient
$C^{(r)}$	Weighing coefficient along the x direction
χ_{ij}^{s}	Symmetric rotation gradient tensor components
ε_{ij}	Strain tensor components
σ_{ij}	Stress tensor components
m_{ij}^{s}	Higher order stress tensor components
W	Work done by sorrounding elastic medium
Π	Strain energy of the structure
n	Number of grid points along the x direction